

*Proteome Res.* Author manuscript; available in PMC 2015 February 04.

Published in final edited form as:

J Proteome Res. 2010 November 5; 9(11): 6025–6032. doi:10.1021/pr100827j.

# Oocyte spindle proteomics analysis leading to rescue of chromosome congression defects in cloned embryos

Zhiming Han<sup>#1</sup>, Cheng-Guang Liang<sup>#1</sup>, Yong Cheng<sup>#1</sup>, Xunbao Duan<sup>2</sup>, Zhisheng Zhong<sup>1</sup>, Santhi Potireddy<sup>1</sup>, Camilo Moncada<sup>2</sup>, Salim Merali<sup>2</sup>, and Keith E. Latham<sup>1,2,#</sup>

<sup>1</sup>The Fels Institute for Cancer Research and Molecular Biology, Temple University School of Medicine

<sup>2</sup>Department of Biochemistry, Temple University School of Medicine

## **Abstract**

Embryos produced by somatic cell nuclear transfer (SCNT) display low term developmental potential. This is associated with deficiencies in spindle composition prior to activation and at early mitotic divisions, including failure to assemble certain proteins on the spindle. The proteindeficient spindles are accompanied by chromosome congression defects prior to activation and during the first mitotic divisions of the embryo. The molecular basis for these deficiencies and how they might be avoided are unknown. Proteomic analyses of spindles isolated from normal metaphase II (MII) stage oocytes and SCNT constructs, along with a systematic immunofluorescent survey of known spindle-associated proteins were undertaken. This was the first proteomics study of mammalian oocyte spindles. The study revealed four proteins as being deficient in spindles of SCNT embryos in addition to those previously identified; these were clathrin heavy chain (CLTC), aurora B kinase, dynactin 4, and casein kinase 1 alpha. Due to substantial reduction in CLTC abundance after spindle removal, we undertook functional studies to explore the importance of CLTC in oocyte spindle function and in chromosome congression defects of cloned embryos. Using siRNA knockdown we demonstrated an essential role for CLTC in chromosome congression during oocyte maturation. We also demonstrated rescue of chromosome congression defects in SCNT embryos at the first mitosis using CLTC mRNA injection. These studies are the first to employ proteomics analyses coupled to functional interventions to rescue a specific molecular defect in cloned embryos.

## Keywords

somatic cell nuclear transfer; meiosis; oogenesis; gene expression; spindle assembly

## Introduction

Previous studies indicated that cloned embryos made by SCNT are defective in spindle formation due to a temporary depletion of spindle proteins as a consequence of the SCNT

<sup>#</sup> These authors contributed equally to this work.

<sup>\*</sup>Correspondence: 3307 North Broad Street, Philadelphia, PA 19140 tel. 215-707-7577 fax 215-707-1454 klatham@temple.edu.

process and a failure to recruit proteins onto the spindles that form after nuclear transfer and at subsequent mitotic divisions<sup>1, 2</sup>. Observed protein deficiencies include calmodulin in mouse clones <sup>1</sup> and NuMA, HSET, and Eg5 in rhesus monkey clones<sup>2</sup>. The calmodulin defect was notable in that this deficiency persisted during early mitotic divisions as well as in the spindle that forms in the oocyte after SCNT<sup>1</sup>. Moreover, the calmodulin defect was a unique property of SCNT constructs, and not observed following blastomere or embryonic stem cell nuclear transfer, indicating an important role of the donor genome in controlling spindle composition<sup>1</sup>.

The spindle composition defects correlate with chromosome congression delays¹ and might limit clone viability by promoting chromosome segregation errors. Knowledge of which spindle proteins are deficient would help guide targeted efforts to rescue chromosome congression defects. Once accomplished, it would be feasible to determine experimentally the degree to which such defects contribute to the limited success of cloning. Meeting this objective poses a significant challenge in that it is necessary to complete a non-biased, global proteomics evaluation of spindle protein composition in order to determine which proteins are deficient and which might constitute a primary defect leading to functional deficiencies. This in turn requires the microsurgical isolation of large numbers of spindles from oocytes and cloned embryos, combined with sensitive analysis of protein populations.

Using a combination of label-free mass spectrophotometric proteomics analysis of isolated spindle-chromosome complexes and an immunofluorescence confocal microscopic survey of spindle composition, we identified proteins deficient in spindles of cloned constructs. Confirmation of the role of one of these, clathrin heavy chain (CLTC), was achieved by experimental depletion of this protein during maturation, which recapitulated the chromosome congression defect; conversely, enhancing expression in cloned embryos rescued the defect. This is the first report wherein a specific molecular deficiency in cloned embryos has been identified by proteomic analysis of a sub-cellular fraction, and then rectified by enhancing expression of a specific target protein.

#### **Materials and Methods**

#### Oocyte collection

Adult female (B6D2)F1 mice (8–12 wk of age) were superovulated by administration of 5 IU of equine chorionic gonadotropin (Calbiochem, San Diego, CA) followed 48 h later by 5 IU of human chorionic gonadotropin (hCG, Sigma-Aldrich, St. Louis, MO). The MII oocytes were isolated at 14–15 h after hCG injection. Cumulus cells were removed by hyaluronidase treatment in HEPES-buffered M2 medium and gentle pipetting. Oocytes were cultured in CZB medium supplemented with 5.5 mM glucose for spindle collection and cloning procedures, as described<sup>3-6</sup>. All studies adhered to procedures consistent with the National Research Council Guide for the Care and Use of Laboratory Animals and were approved by the Institutional Animal Care and Use Committee at Temple University.

## ooSCC and pmSCC collection

Spindle chromosome complexes from MII stage oocytes (ooSCCs) were removed using a narrow-bore pipette attached to a piezo pipette driver as described<sup>6,7</sup>. This was performed in HEPES-buffered CZB medium (HCZB) supplemented with 5.5 mM glucose and 2.5  $\mu$ g/ml cytochalasin B (Sigma-Aldrich). Isolated ooSCCs and the SCC-depleted ooplasm of MII oocytes were collected separately in 1.5 ml microtubes and stored at  $-70^{\circ}$ C. To obtain spindle-chromosome complexes formed after SCNT (pseudomeiotic SCCs or pmSCCs), SCNT constructs were prepared by injection of cumulus cell nuclei into SCC-depleted oocytes, as described<sup>6</sup>. After 2 h culture in CZB medium supplemented with 5.5 mM glucose, the pmSCCs were collected and stored as above. The overall efficiency of recovery of pmSCCs was about 80%.

#### SDS PAGE Separation and In-Gel Trypsin Digestion

Each of three samples (100 SCC-depleted ooplasms from MII oocytes, 5000 pmSCCs from cloned constructs and 5000 ooSCCs from MII oocytes) was diluted at a 1:2 ratio with Laemmli sample buffer (BioRad, Hercules, CA) containing 5%  $\beta$ -mercaptoethanol, heated for 10 min at 90°C and loaded onto a 10-14% polyacrylamide gel. Electrophoresis was performed using a mini Protean II system (BioRad) at 200 V for 45 min. Separation was confirmed by staining with SimplyBlue SafeStain (Invitrogen, Carlsbad, CA). Each of the three sample lanes was sliced into 20 sections, and each section further cut into ~1 mm³ pieces. The gel pieces were treated with 10 mM DTT in 50 mM ammonium bicarbonate for 30 min at 37°C and the proteins then alkylated with 50 mM iodoacetamide in 50 mM ammonium bicarbonate for 30 min at room temperature in the dark. After treatment with 50% (v/v) acetonitrile in 50 mM bicarbonate and dehydration with pure acetonitrile, approximately 40  $\mu$ l 12.5  $\mu$ g/ $\mu$ l trypsin in 50 mM ammonium bicarbonate solution was added to cover the gel pieces. The trypsin digestion, peptide extraction, and sample cleanup were performed as described8.

## Nano-LC-IT MS and Data Analysis

The desalted peptides were dried in a vacuum centrifuge and resolubilized in 30  $\mu$ l of 0.1% (vol/vol) trifluoroacetic acid. The tryptic peptide sample was loaded onto a 2  $\mu$ g capacity peptide trap (CapTrap; Michrom Bioresources) separated by a C18 capillary column (15 cm 75  $\mu$ m, Agilent) at 300 nl/min delivered by an Agilent 1100 LC pump. A mobile-phase gradient was run using mobile phase A (1% acetonitrile/0.1% formic acid) and B (80% acetonitrile/0.1% formic acid) from 0 to 10 min with 0-15% B followed by 10-60 min with 15-60 % B and 60-65 min with 60-100 % B. Nanoelectrospray ionization (ESI) tandem MS was performed using a HCT Ultra ion trap mass spectrometer (Bruker). ESI was delivered using a distal-coating spray Silica tip (ID 20  $\mu$ M, tip inner ID 10  $\mu$ M, New Objective) at a spray voltage of -1300 V. Using an automatic switching between MS and MS/MS modes, MS/MS fragmentation was performed on the two most abundant ions on each spectrum using collision –induced dissociation with active exclusion (excluded after two spectra, and released after 2 min). The complete system was fully controlled by HyStar 3.1 software.

Mass spectra (MS) processing was performed using Mascot Distiller (Version 2.3.0.0) with search and quantitation toolbox options. The generated de-isotoped peak list was submitted

to an in-house Mascot server 2.2 for searching against the Swiss-Prot database (version 56.6 of 16-Dec-2008, 405506 sequences). Mascot search parameters were set as follows: species Mus musculus (20413 sequences); enzyme, trypsin with maximal 1 missed cleavage; fixed modification, cysteine carbamidomethylation; variable modification, methionine oxidation; 0.50 Da mass tolerance for precursor peptide ions; and 0.6 Da for MS/MS fragment ions. All peptide matches were filtered using an ion score cutoff of 10. The following two criteria were used to evaluate protein identification: one peptide with ion score 50, two or more peptides with at least one ion score 32 (p < 0.05 threshold) and the cumulative Mascot scores 50; for all the proteins with cumulative MOWSE scores 50 and 80, the theoretical and experimental gel molecular weights had to be consistent. When these criteria were used to search against a reversed decoy Swiss-Prot database, there was no false positive match (false discovery < 0.5%). For added stringency, proteins with scores above 100 were used for comparisons between samples. For protein quantification, a combination of peptide number and modified peptide counting, APEX, was used  $^{9, 10}$ .

## siRNA and mRNA injections

Cltc siRNAs were purchased from Sigma-Aldrich. A combination of two siRNAs was used: Oligo#1246094: 5'CCAUACAGAAGACCGUUAA[dT][dT]; Oligo#1246095: 5'UUAACGGUCUUCUGUAUGG[dT][dT]. The siRNAs were injected into GV stage (B6D2)F1 oocytes as described<sup>11</sup> and the oocytes cultured in CZB with IBMX for 20 h. Oocytes were then transferred to maturation medium without IBMX for 16 h. Oocytes were checked for the first polar body (PB1) extrusion and collected for western blot analysis or fixed for immunostaining. MII stage oocytes were fixed and processed for visualizing spindles and chromosomes or processed for western blotting. For rescue experiments, the human full length CLTC cDNA construct (Open Biosystems, clone ID#6045540, GenBank ID-BC054489) with 99% amino acid sequence identity to mouse *Cltc* was used. The human CLTC mRNA is 6529 bp long with 228-5255 bp corresponding to the coding sequence. Restriction enzyme digestion and sequencing were performed to confirm the sequence of the insert. Transcription with the Ambion mMESSAGE mMACHINE transcription kit (Ambion, cat # AM1344) was performed on 1 µg of Hind III linearized plasmid DNA. mRNA was synthesized by transcription using the SP6 promoter in the pCMV-SPORT6 vector and then subjected to poly(A) tailing using Ambion kit (Ambion, cat# AM1350). Polyadenylated mRNA was precipitated using LiCl<sub>2</sub>. The concentration and quality of RNA were checked using a spectrophotometer and formaldehyde gel electrophoresis. The mRNA was injected into oocytes at 1 h after ooSCC removal. Each oocyte was injected with 1 pl mRNA solution, which was diluted in 0.1 mM EDTA, to deliver approximately 1 fmol CLTC mRNA, judged to yield a comparable protein level to that of in vivo late 1-cell embryos.

#### **Immunostaining**

Oocytes and embryos were incubated in acidic tyrode solution (pH 2.5) for 10-15 seconds to remove the zona pellucida. After washing at least 4 times in M2 medium, they were fixed in 4% paraformaldehyde (Electron Microscopy Sciences, Hatfield, PA) in PBS at room temperature for 50 minutes and permeabilized with 0.5% Triton X-100 (Bio Rad; Richmond, CA) for 2 h at room temperature. After blocking with 1% BSA in washing buffer

[PBS supplemented with 1/1,000 Tween-20 (BioRad; Hercules, CA) and 1/10,000 Triton X-100] for 1 h at room temperature, samples were incubated with primary antibody at 4°C overnight. The sources and dilutions of primary antibodies are listed in Supplemental Table 1. After three washes, samples were incubated with Donkey anti-mouse, anti-rabbit or antigoat IgG (H+L) secondary antibody, FITC-conjugated (1:100; Jackson ImmunoResearch Laboratories; West Grove, PA) for 1 h at room temperature and again washed three times. Samples were incubated with propidium iodide (1:50 in washing buffer) for 5 min, washed once, and mounted on slides using Vectashield (Burlingame, CA) mounting medium. Cells were imaged using confocal laser microcopy (Leica TCS SP5) using 488 nm (Argon) and 568 nm (Krypton) lasers for excitation of FITC and PI fluorescence, respectively. Images of optical sections were captured at 1  $\mu$ m intervals. Images were analyzed with the Leica LAS AF software. MII plate thickness was measured by drawing two lines at the edges of the red region (PI staining) and perpendicular to the spindle axis defined by the green region (TUBB1 staining). The distance between these two lines was used as the MII plate thickness.

#### Western blot

Western blotting was performed as described<sup>1</sup> except that a 4%-15% gradient gel (Bio-Rad) was used. Blots were processed to visualize CLTC (180 kD) and GAPDH (37 kD).

## Results

## Proteomics analysis of oocyte and cloned construct spindles

We undertook the first ever proteomics analysis of mammalian oocyte spindles. This analysis began with the manual isolation of 5000 oocyte spindle-chromosome complexes (ooSCCs) from normal MII stage mouse oocytes, and 5000 SCCs recovered from cloned constructs at 2 h after SCNT (pmSCCs; 80% efficiency starting with 6225 cloned constructs total). These SCCs were compared to each other and to an ooplast lysate in protein composition by gel electrophoresis liquid chromatography mass spectroscopy (GeLC MS/MS) combined with absolute protein expression estimates (APEX) and peptide counts. These methods detected over 200 proteins in each of the SCC samples and over 400 in the ooplasm sample. Of these, 64 were enriched in ooSCC compared to ooplasm and 42 were enriched in pmSCC compared to ooplasm. To compare ooSCCs and pmSCCs, we selected highly significant identified proteins (MOWSE scores of 100 or greater, Table 1) for comparison and found 25 with higher abundance in the ooSCCs and 6 higher in pmSCCs, of which 19 were only detected in the ooSCC sample (Table 2). Clathrin heavy chain yielded the highest score and was selected for further study. In parallel, we used immunofluorescence confocal microscopy to survey proteins expected to be associated with SCCs but excluded previously identified chromosome-associated proteins<sup>12-14</sup> (Table S1). These combined approaches revealed 4 proteins with differential staining in pmSCC vs. ooSCC: clathrin heavy chain (CLTC); aurora B (AURKB), dynactin 4 (DCTN4), and casein kinase 1 alpha (CSNK1A1) (Fig. 1A). All four proteins displayed greatly reduced presence in pmSCCs of cloned constructs compared to normal ooSCCs, and none achieved intense pmSCC staining. While some proteins accumulated on the pmSCC further with continued incubation to 3 h, they remained reduced relative to ooSCC. Reduced presence of these

proteins revealed by immunofluorescence (Fig. 1A) was associated with poor chromosome assembly on the metaphase plate. Interestingly, even when tetraploid SCNT constructs were made by injecting donor cell nuclei into oocytes without prior removal of the ooSCCs, all four proteins showed a reduced presence in the pmSCCs that formed (Fig 2). The reduction in clathrin heavy chain (CLTC) was less in pmSCCs of tetraploids than in conventional diploid SCNT embryos, suggesting that ooSCC removal prior to donor nuclei injection depletes much of the CLTC from the oocyte. Of the other three affected proteins, CSNK1A1 and AURKB remained severely deficient in pmSCCs of tetraploids even 3 h after SCNT while DCTN4 was similar to CLTC in that it increased on the pmSCC during this period.

CLTC, DCTN4, and AURKB are clearly associated with the spindle microtubules, whereas CSNK1A1 is associated with the condensed chromosomes. CLTC was most notable as being prominent amongst proteins identified by the GeLC MS/MS analysis, intense signal on ooSCCs (73 relative intensity units compared to 2 and 48 for AURKB and DCTN4, respectively), and the greatest apparent enrichment in the SCC compared to ooplasm staining intensity in MII oocytes (Fig. 1A). Western blot analysis (Fig. 1B) confirmed a significant depletion of CLTC from oocytes after SCC removal, an effect that persisted during the 3 h incubation. Recovery of CLTC expression on western blot was hastened by the presence of a donor cell nucleus in SCNT constructs. For these reasons, CLTC was examined in greater detail through functional studies.

## Role of CLTC in oocyte spindle function

The chromosome congression defect is a prominent feature of SCNT constructs  $^1$  (Figs 1, 2). To determine whether a CLTC deficiency alone affects chromosome congression, we reduced CLTC expression in MII oocytes using siRNA (Fig. 3 A,B). Injection of GV stage oocytes with siRNA for *Cltc* followed by in vitro maturation resulted in a nearly 4-fold increase in the number of MII stage ooSCC showing lagging chromosomes (p < 0.01) and a 34.9% increase in the thickness of the MII plate (p < 0.05) (Fig. 3C). There was no effect on maturation or polar body extrusion (Fig. 3C).

#### Role of CLTC in chromosome congression failure in clone development

The identification of the CLTC defect and the determination of its role in normal meiotic spindle function provided an opportunity to test whether chromosome congression defects in clones are related to deficient CLTC assembly on the SCC. Our approach was to test whether an augmented supply of CLTC protein could enhance chromosome congression, which is observed both in the pmSCC that forms immediately after SCNT and in the spindle of the subsequent mitotic division. It is also noted that SCC defects in the pmSCC that forms immediately after SCNT and before activation is likely of little biological consequence, because polar body extrusion is prevented during the activation step so that no chromosome loss can occur. To avoid negative effects of either in vitro maturation or delaying SCNT procedure to allow enhanced CLTC accumulation before SCNT, and to address the functionally more meaningful defects in cloned embryos, we opted to test whether enhanced CLTC expression could improve chromosome congression at the first mitotic division in SCNT embryos. Embryos with defective chromosome congression were defined as those with lagging chromosome(s). Injection of *CLTC* mRNA into SCC-depleted ooplasts

increased CLTC expression in 1-cell stage SCNT constructs (Fig. 4A) and reduced the incidence of congression defects at the first mitosis in terms of the fraction of embryos showing lagging chromosomes (Fig. 4B,C) (p < 0.01), and the number of lagging chromosomes (1.85+0.87 for SCNT versus 1.29+0.47 for SCNT+mRNA, p < 0.05) per embryo.

Previous authors have suggested that chromosome congression failure and mitotic errors could be a significant component in the limited term development of cloned embryos<sup>2</sup>. It would follow that if these defects were overcome, this could enhance developmental outcome. The successful suppression of these chromosome congression defects in SCNT embryos provided the opportunity to test whether overcoming such defects would indeed improve cloning outcome. To test whether term development could be enhanced in SCNT constructs by *CLTC* mRNA injection, treated and untreated embryos were transferred to surrogate foster mothers for development (Table 3). *CLTC* mRNA injection did not promote increased development to term (3.6 versus 2.9% term development for 299 control and 278 *CLTC* mRNA injected constructs, respectively).

## **Discussion**

This is the first study to undertake a proteomics analysis of meiotic spindles from oocytes of any mammal, and the first study to undertake a systematic analysis of SCCs from cloned embryos. This is a significant accomplishment, as it entailed the microsurgical isolation of large numbers of SCCs and extensive immunofluorescence analysis coupled with sensitive methods of protein detection and comparison. The result has been the identification of four additional proteins that are deficient in SCCs of SCNT embryos. We demonstrate that CLTC plays a role in normal meiosis. We also show for the first time that enhanced CLTC expression can overcome chromosome congression defects in cloned embryos.

Known more widely for its role in endocytosis and membrane trafficking, the role of CLTC in mitosis has emerged relatively recently <sup>15-18</sup>. Studies of CLTC role in mitosis revealed defects in some cells following CLTC knockdown with siRNA <sup>16-18</sup> and knockdown of GAK, a clathrin regulator <sup>17</sup>. More recent studies, however, indicate that the requirement for CLTC in mitosis may be cell-type dependent <sup>19</sup>. Our studies reveal that CLTC also plays a critical role in chromosome congression during mammalian meiosis. While this paper was in preparation, another study was published demonstrating a role for clathrin in spindle function in pig oocytes <sup>20</sup>. These results highlight the need for further study of the role of CLTC in this process, and its effects on fertility and evolution. It is intriguing that other proteins that associate with CLTC and/or are involved in endocytosis populate our list of differences observed by MS; these include NSF, CLTB, and VAPA. Additionally, we note the reduction in tubulin isoforms in the spindle, both in the MS results and in the immunofluorescence visualization of microtubule density, which is affected by CLTC triskelia binding (Fig. 3A). Collectively, these results point to an interesting, emerging connection between proteins involved in endocytosis and meiosis.

The discovery of the role of CLTC in promoting chromosome congression may lead to new strategies for enhancing human oocyte quality and success of assisted reproduction.

Chromosome congression defects are prominent amongst oocytes as women's age increases<sup>21</sup>. Future development of methods for in vitro oocyte maturation might be accompanied by CLTC augmentation to improve chromosome congression.

We show that defects in CLTC expression underlie the chromosome congression deficiency in cloned embryos. CLTC expression is dramatically reduced by SCC removal, and CLTC expression recovers more quickly with a genome present. These results are similar to previous results for calmodulin<sup>1</sup>, thus indicating that a general feature of SCC formation is that the presence of chromatin associated with the incipient SCC promotes accelerated accumulation of SCC proteins. This may be in part due to stabilization of these proteins as they become associated with the spindle. However, the persistence of reduced staining intensity on the pmSCC indicates that other mechanisms may control protein accumulation.

Our study is the first wherein a proteomics analysis was applied to diagnose and correct a specific molecular defect in cloned embryos. This led to rescue of a specific cellular abnormality (chromosome congression defect) through the targeted augmentation of a specific molecular component of the cell. This successful application of proteomics methods to limited amounts of material isolated manually from mouse oocytes, combined with the subsequent functional complementation, illustrate the sensitivity and power of such approaches to guide successful interventions.

Based on our proteomics analysis, additional proteins are defective in pmSCC of SCNT constructs. Further studies of the functions of these proteins in oocytes and embryos and how they interact with each other should illuminate the mechanisms that control spindle formation and chromosome assembly. For example, the mechanism by which chromatin exerts an influence on spindle formation and functions remains to be identified.

Our results provided an opportunity to test whether enhanced chromosome congression could improve cloning outcome. Injecting the *CLTC* mRNA into cloned constructs improved chromosome congression but did not lead to an increase in term development. It is interesting to note that cloning by transfer of M-phase genomes has not dramatically increased cloning efficiency<sup>22, 23</sup>. Because these approaches employ well-formed SCCs as donor material, this suggests that other significant barriers to cloning exist, and that multiple problems likely must be overcome to enhance term development in clones. Other defects to be addressed likely include limited reprogramming in gene expression, limited establishment of pluripotency in the early embryo, and unique in vitro culture requirements of cloned embryos<sup>24-26</sup>. It is possible that correction of spindle defects together with enhancing reprogramming activities will ultimately improve cloning outcomes. Combined approaches that address multiple aspects of cloned embryo biology should prove valuable for the production of cloned animals for agricultural, conservation, and biopharmaceutical purposes, and for the production of stem cells for therapeutic applications.

## **Supplementary Material**

Refer to Web version on PubMed Central for supplementary material.

## **Acknowledgments**

This work was supported by a grant from the National Institute of Child Health and Human Development (NIH/NICHD HD52788).

#### References

 Miyara F, Han Z, Gao S, Vassena R, Latham KE. Non-equivalence of embryonic and somatic cell nuclei affecting spindle composition in clones. Dev Biol. 2006; 289(1):206–17. [PubMed: 16310175]

- Simerly C, Dominko T, Navara C, Payne C, Capuano S, Gosman G, Chong KY, Takahashi D, Chace C, Compton D, Hewitson L, Schatten G. Molecular correlates of primate nuclear transfer failures. Science. 2003; 300(5617):297. [PubMed: 12690191]
- 3. Chung YG, Ratnam S, Chaillet JR, Latham KE. Abnormal regulation of DNA methyltransferase expression in cloned mouse embryos. Biol Reprod. 2003; 69(1):146–53. [PubMed: 12606374]
- Gao S, Chung YG, Williams JW, Riley J, Moley K, Latham KE. Somatic cell-like features of cloned mouse embryos prepared with cultured myoblast nuclei. Biol Reprod. 2003; 69(1):48–56. [PubMed: 12606377]
- Gao S, McGarry M, Latham KE, Wilmut I. Cloning of mice by nuclear transfer. Cloning Stem Cells. 2003; 5(4):287–94. [PubMed: 14733747]
- Han Z, Vassena R, Chi MM, Potireddy S, Sutovsky M, Moley KH, Sutovsky P, Latham KE. Role of glucose in cloned mouse embryo development. Am J Physiol Endocrinol Metab. 2008; 295(4):E798–809. [PubMed: 18577693]
- Wakayama T, Perry AC, Zuccotti M, Johnson KR, Yanagimachi R. Full- term development of mice from enucleated oocytes injected with cumulus cell nuclei. Nature. 1998; 394(6691):369–74.
   [PubMed: 9690471]
- 8. Duan X, Kelsen SG, Merali S. Proteomic analysis of oxidative stress- responsive proteins in human pneumocytes: insight into the regulation of DJ-1 expression. J Proteome Res. 2008; 7(11):4955–61. [PubMed: 18817430]
- Cravatt BF, Simon GM, Yates JR 3rd. The biological impact of mass-spectrometry-based proteomics. Nature. 2007; 450(7172):991–1000. [PubMed: 18075578]
- Lu P, Vogel C, Wang R, Yao X, Marcotte EM. Absolute protein expression profiling estimates the relative contributions of transcriptional and translational regulation. Nat Biotechnol. 2007; 25(1): 117–24. [PubMed: 17187058]
- 11. Stein P. Microinjection of dsRNA into fully-grown mouse oocytes. Cold Spring Harb Protoc. 2009; 2009(1):pdb prot5132. [PubMed: 20147027]
- 12. Nousiainen M, Sillje HH, Sauer G, Nigg EA, Korner R. Phosphoproteome analysis of the human mitotic spindle. Proc Natl Acad Sci U S A. 2006; 103(14):5391–6. [PubMed: 16565220]
- 13. Sauer G, Korner R, Hanisch A, Ries A, Nigg EA, Sillje HH. Proteome analysis of the human mitotic spindle. Mol Cell Proteomics. 2005; 4(1):35–43. [PubMed: 15561729]
- Wong J, Nakajima Y, Westermann S, Shang C, Kang JS, Goodner C, Houshmand P, Fields S, Chan CS, Drubin D, Barnes G, Hazbun T. A protein interaction map of the mitotic spindle. Mol Biol Cell. 2007; 18(10):3800–9. [PubMed: 17634282]
- 15. Lin CH, Hu CK, Shih HM. Clathrin heavy chain mediates TACC3 targeting to mitotic spindles to ensure spindle stability. J Cell Biol. 2010; 189(7):1097–105. [PubMed: 20566684]
- Royle SJ, Bright NA, Lagnado L. Clathrin is required for the function of the mitotic spindle. Nature. 2005; 434(7037):1152–7. [PubMed: 15858577]
- 17. Shimizu H, Nagamori I, Yabuta N, Nojima H. GAK, a regulator of clathrin-mediated membrane traffic, also controls centrosome integrity and chromosome congression. J Cell Sci. 2009; 122(Pt 17):3145–52. [PubMed: 19654208]
- 18. Tahara H, Yokota E, Igarashi H, Orii H, Yao M, Sonobe S, Hashimoto T, Hussey PJ, Shimmen T. Clathrin is involved in organization of mitotic spindle and phragmoplast as well as in endocytosis in tobacco cell cultures. Protoplasma. 2007; 230(1-2):1–11. [PubMed: 17351731]

 Borlido J, Veltri G, Jackson AP, Mills IG. Clathrin is spindle-associated but not essential for mitosis. PLoS One. 2008; 3(9):e3115. [PubMed: 18769625]

- Holzenspies JJ, Roelen BA, Colenbrander B, Romijn RA, Hemrika W, Stoorvogel W, van Haeften T. Clathrin is essential for meiotic spindle function in oocytes. Reproduction. 2010; 140(2):223–33. [PubMed: 20522479]
- 21. Hassold T, Hunt P. Maternal age and chromosomally abnormal pregnancies: what we know and what we wish we knew. Curr Opin Pediatr. 2009; 21(6):703–8. [PubMed: 19881348]
- 22. Amano T, Tani T, Kato Y, Tsunoda Y. Mouse cloned from embryonic stem (ES) cells synchronized in metaphase with nocodazole. J Exp Zool. 2001; 289(2):139–45. [PubMed: 11169501]
- 23. Ono Y, Shimozawa N, Ito M, Kono T. Cloned mice from fetal fibroblast cells arrested at metaphase by a serial nuclear transfer. Biol Reprod. 2001; 64(1):44–50. [PubMed: 11133657]
- 24. Gao S, Latham KE. Maternal and environmental factors in early cloned embryo development. Cytogenet Genome Res. 2004; 105(2-4):279–84. [PubMed: 15237216]
- 25. Latham KE. Early and delayed aspects of nuclear reprogramming during cloning. Biol Cell. 2005; 97(2):119–32. [PubMed: 15656778]
- 26. Wilmut I, Paterson L. Somatic cell nuclear transfer. Oncol Res. 2003; 13(6-10):303–7. [PubMed: 12725518]

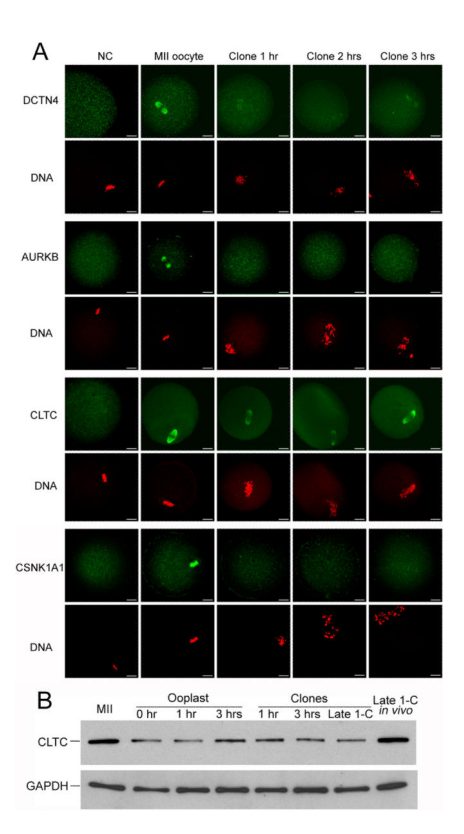


Fig 1. Expression of proteins that show differences between ooSCCs and pmSCCs. (A) Confocal immunofluorescent analysis. Green, spindle protein (DCTN4, AURKB, CLTC, CSNK1A1). red, DNA. Clone 1 h, 2 h, 3 h represents time after SCNT. The scale bar =  $10 \mu m$ . (B) Western blot analysis of CLTC in oocytes, fertilized embryos and clone constructs.

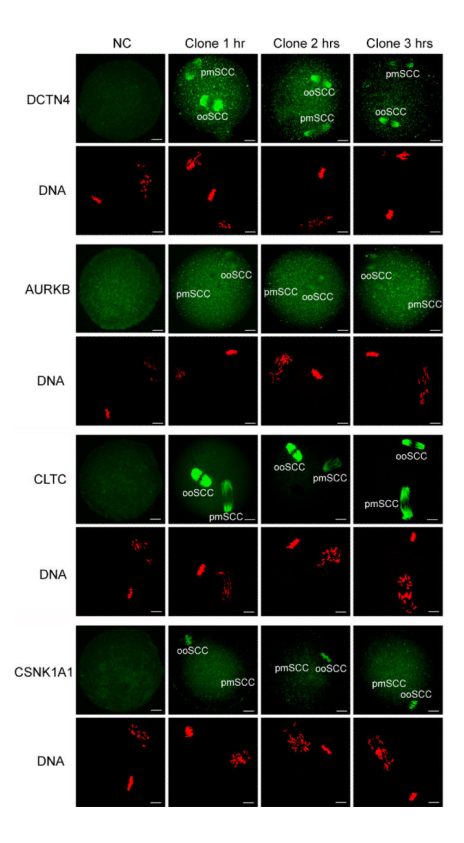


Fig 2. Confocal microscopic imaging of tetraploid embryos stained with antibody for DCTN4, AURKB, CLTC and Casein kinase 1 alpha. Green, spindle proteins, red, DNA. Clone 1 h, 2 h, 3 h represents recovery time after cumulus nuclei injection. The spindles corresponding to the ooSCC and pmSCC are indicated. The scale bar =  $10 \, \mu m$ 

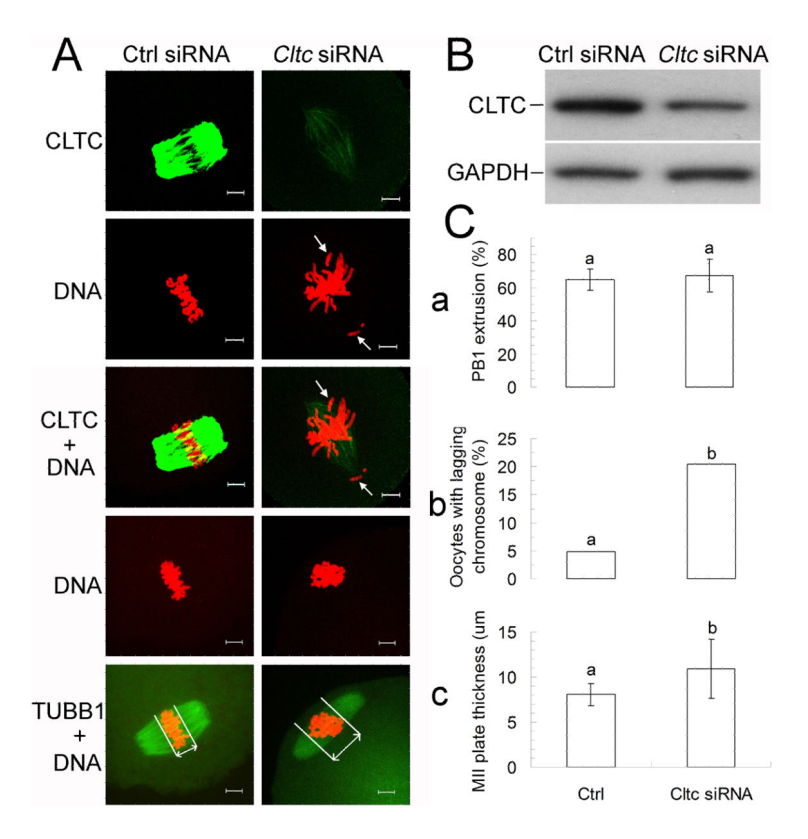
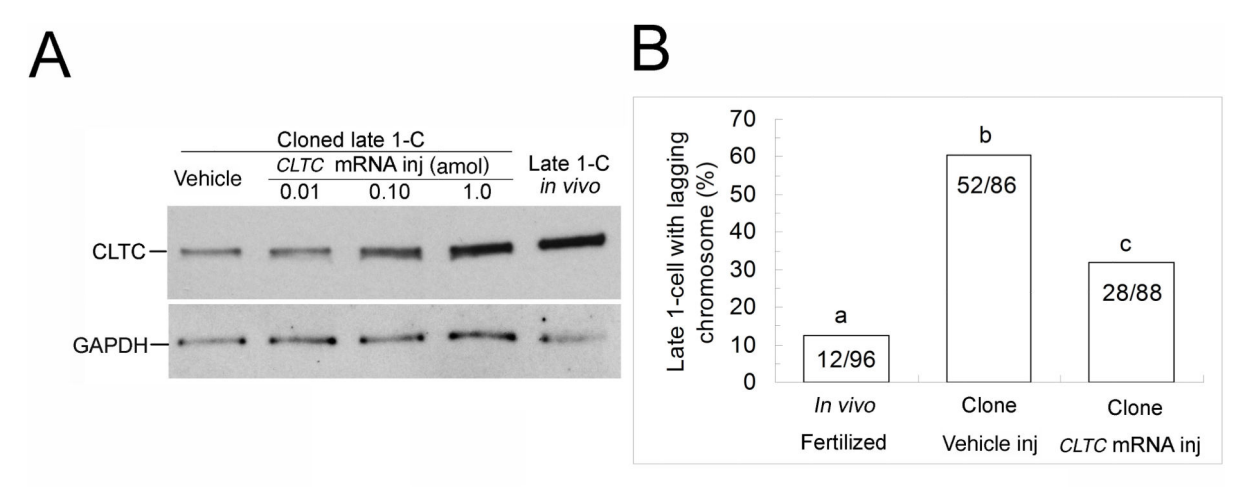


Fig 3. Effect of *Cltc* siRNA on oocyte maturation and chromosome congression. (A), Confocal microscopic imaging of knockdown effect of *Cltc* siRNA. Green: CLTC (row 1 and 3) and beta tubulin (row 5), Red: DNA. Lagging chromosomes are indicated by arrows. The scale bar = 5  $\mu$ m. (B), Western blot analysis of knockdown effect of *Cltc* siRNA. Control group was injected with non-specific siRNA. GAPDH was used as a loading control. Each lane received 100 oocytes. (C), Effect of CLTC knockdown on oocyte maturation (a), chromosome misalignment (b) and MII plate thickness (c). T-test was used to test significance of difference for oocyte maturation and MII plate thickness (P < 0.05). Chi square test was used to test significance of difference for chromosome misalignment (P < 0.01).



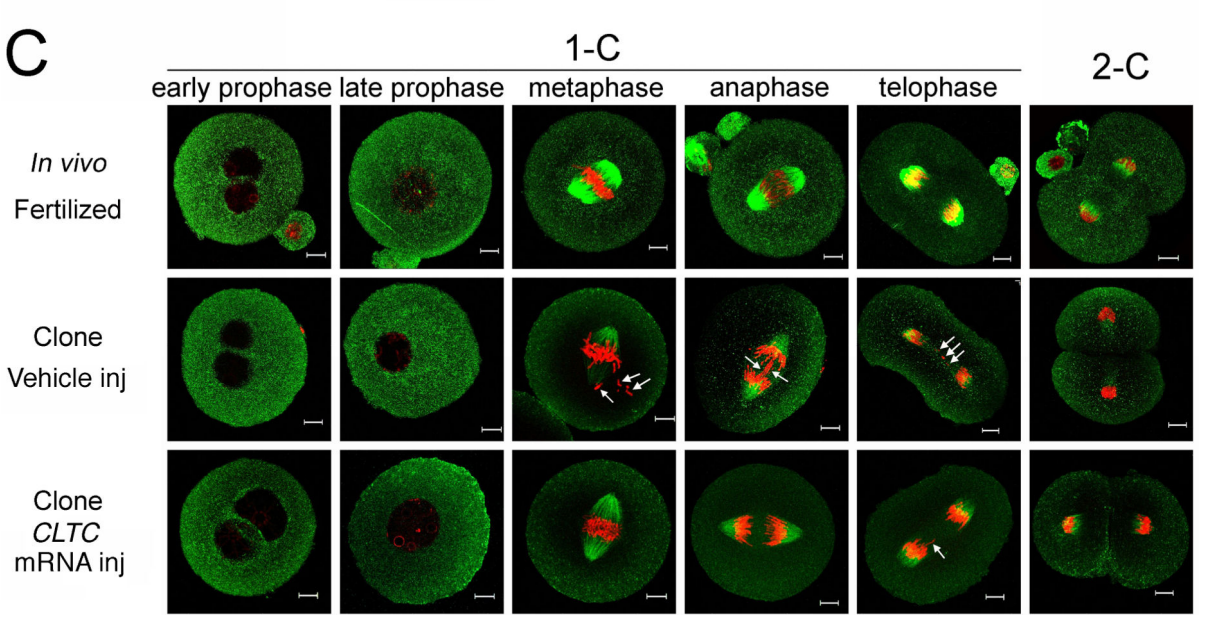


Fig 4.

Effect of *CLTC* mRNA on embryo development. (A) Western blot analysis of CLTC in cloned or fertilized late 1-cell embryos uninjected or injected with different amounts of *CLTC* mRNA at 1 h after SCC removal. 0.1mM EDTA was injected as vehicle injection control. GAPDH was used as loading control. Each lane received 20 embryos of indicated type. (B): Rescue effect of *CLTC* mRNA on the percentage of late 1-cell stage embryos with lagging chromosome(s). Number of embryos with lagging chromosome and total embryos are indicated in each bar. Chi square was used to test the significance of difference. Bars with different letter are significantly different (P < 0.01). (C) Confocal microscopic imaging of rescue effect of *CLTC* mRNA in 1-cell stage embryos. 1.0 fmol *CLTC* mRNA was injected into ooplasm at 1 hour after SCC removal. Embryos were fixed at 1-cell to 2-cell stage. Left to right: early prophase, late prophase, metaphase, anaphase, telophase and early 2-cell stage. First row: fertilized embryos; Second row, cloned embryos injected with 0.1

mM EDTA vehicle control; Third row, cloned embryos injected with  $\it CLTC$  mRNA. Green, CLTC; Red, DNA. Lagging chromosomes were indicated by arrows. The scale bar = 10  $\mu m$ .

Han et al. Page 16

Table 1

Proteins enriched in the ooSCC or pmSCC samples compared to SCC-depleted ooplasm

a. Proteins enriched in ooSCC						
Symbol	Protein name	Score	MW (Da)	Pep		
ACTB	Actin, cytoplasmic 1	969	41710	46		
ACTN1	Alpha-actinin-1	262	103004	5		
ACTN4	Alpha-actinin-4	625	104911	12		
ARC1B	Actin-related protein 2/3 complex subunit 1B	132	41123	3		
ARP2	Actin-related protein 2	278	44732	8		
ARP3	Actin-related protein 3	255	47327	7		
ARPC2	Actin-related protein 2/3 complex subunit 2	242	34336	10		
CAPZB	F-actin-capping protein subunit beta	298	31326	7		
CLTB	Clathrin light chain B	206	25156	6		
CLTC	Clathrin heavy chain 1	2741	191435	95		
DCLK2	Serine/threonine-protein kinase DCLK2	114	82927	2		
DLGAP5	Disks large-associated protein 5	378	90141	10		
GLRX1	Glutaredoxin-1	181	11863	4		
GTSE1	G2 and S phase-expressed protein 1	123	78703	3		
H1FOO	Histone H100	192	32203	5		
H2A1F	Histone H2A type 1-F	119	14153	8		
H2B1A	Histone H2B type 1-A	150	14228	8		
H2B1B	Histone H2B type 1-B	212	13944	13		
HIST4H4	Histone cluster 4, H4	424	11360	15		
HSP74	Heat shock 70 kDa protein 4	594	94073	14		
IMB1	Importin subunit beta-1	231	97090	7		
KIF2C	Kinesin-like protein KIF2C	119	81034	3		
LEGLB	Galectin-related protein B	112	18258	3		
MTAP4	Microtubule-associated protein 4	130	117357	5		
MRLC2	Myosin regulatory light chain MRLC2	264	19767	9		
MYO18A	Myosin-XVIIIa	233	232611	5		
MYL6	Myosin light polypeptide 6	365	16919	8		
NLRP9C	NACHT, LRR and PYD domains-containing protein 9C	163	115646	4		
NEXN	Nexilin	343	72094	8		
TACC3	Transforming acidic coiled-coil-containing protein 3	497	70583	16		
TUBA1A	Tubulin alpha-1A chain	823	50104	29		
TUBA1C	Tubulin alpha-1C chain	934	49877	36		
TUBA4A	Tubulin alpha-4A chain	565	49892	20		
TUBB2A	Tubulin beta-2A chain	1154	49875	43		
TUBB2C	Tubulin beta-2C chain	1138	49799	43		
TUBB3	Tubulin beta-3 chain	840	50386	28		
TUBB5	Tubulin beta-5 chain	1008	49639	41		
TUBB6	Tubulin beta-6 chain	801	50058	23		

a. Proteins enriched in ooSCC							
Symbol	Protein name	name Score MW (Da)		Pep			
VAPA	Vesicle-associated membrane protein, associated protein A	131	27837	3			

b. Proteins enriched in pmSCC

Symbol	Protein name	Score	MW (Da)	Pep
ARP2	Actin-related protein 2	194	44732	6
ARP3	Actin-related protein 3	200	47327	6
ARPC2	Actin-related protein 2/3 complex subunit 2	160	34336	5
CLTB	Clathrin light chain B	164	25156	4
CLTC	Clathrin heavy chain 1	2429	191435	71
DCLK2	Serine/threonine-protein kinase DCLK2	183	82927	4
DLGAP5	Disks large-associated protein 5	124	90141	4
DNMT3L	DNA (cytosine-5)-methyltransferase 3-like	187	47962	4
ARHGDIA	Rho GDP-dissociation inhibitor 1	173	23393	4
H1FOO	Histone H100	275	32203	7
H2A1F	Histone H2A type 1-F	118	14153	7
H2B1B	Histone H2B type 1-B	243	13944	12
HIST4H4	Histone cluster 4, H4	463	11360	20
NLRP9C	NACHT, LRR and PYD domains-containing protein 9C	165	115646	3
NEXN	Nexilin	283	72094	6
NSF	Vesicle-fusing ATPase	240	82561	7
SMARCA5	$SWI/SNF\mbox{-related},$ matrix-associated, actin-dependent regulator of chromatin, subfamily A, member 5	123	121550	6
TACC3	Transforming acidic coiled-coil-containing protein 3	419	70583	17
TUBA1C	Tubulin alpha-1C chain	791	49877	30
TUBB2A	Tubulin beta-2A chain	1224	49875	42
TUBB2C	Tubulin beta-2C chain	1139	49799	41
TUBB3	Tubulin beta-3 chain	822	50386	26
TUBB5	Tubulin beta-5 chain	1004	49639	38

Score, MASCOT score; MW, molecular weight; Pep, peptide matches, number of peptides identified to protein. Proteins with scores over 100 were included.

Table 2

Proteins differing between ooSCC and pmSCC

a. Proteins with expression ooSCC > pmSCC							
Symbol	Name	Score	MW (Da)	Pep	ooSCC/pmSCC		
ACTB	Actin, cytoplasmic 1	969	41710	46			
ACTN1	Alpha-actinin-1	262	103004	5			
ACTN4	Alpha-actinin-4	625	104911	12			
ACTR2	actin-related protein 2 homolog	278	44732	8	1.33		
ARPC2	Actin-related protein 2/3 complex subunit 2	242	34336	10	2		
CAPZB	F-actin-capping protein subunit beta	298	31326	7			
CLTB	Clathrin light chain B	206	25156	6	1.5		
CLTC	Clathrin heavy chain 1	2741	191435	95	1.34		
DLGAP5	Disks large-associated protein 5	378	90141	10	2.5		
GLRX1	Glutaredoxin-1	181	11863	4			
GTSE1	G2 and S phase-expressed protein 1	123	78703	3			
H2B1A	Histone H2B type 1-A	150	14228	8			
HSP74	Heat shock 70 kDa protein 4	594	94073	14			
KPNB1	Importin subunit beta-1	231	97090	7			
KIF2C	Kinesin-like protein KIF2C	119	81034	3			
LEGLB	Galectin-related protein B	112	18258	3			
MTAP4	Microtubule-associated protein 4	130	117357	5			
MRLC2	Myosin regulatory light chain MRLC2	264	19767	9			
MYO18A	Myosin-XVIIIa	233	232611	5			
MYL6	Myosin light polypeptide 6	365	16919	8			
TUBA1A	Tubulin alpha-1A chain	823	50104	29			
TUBA1C	Tubulin alpha-1C chain	934	49877	36	1.2		
TUBA4A	Tubulin alpha-4A chain	565	49892	20			
TUBB6	Tubulin beta-6 chain	801	50058	23			
VAPA	Vesicle-associated membrane protein, associated protein A	131	27837	3			

b. Proteins with expression pmSCC > ooSCC							
Symbol	Protein name	Score	MW (Da)	Pep	ooSCC/pmSCC		
DCLK2	Doublecortin like kinase 2	183	82927	4	0.4		
DNMT3L	DNA (cytosine-5)-methyltransferase 3-like	187	47962	4			
ARHGDIA	Rho GDP-dissociation inhibitor 1	173	23393	4			
H1FOO	Histone H100	275	32203	7	0.71		
NSF	Vesicle-fusing ATPase	240	82561	7			
SMARCA5	SWI/SNF-related matrix-associated actin-dependent regulator of chromatin subfamily A member 5	123	121550	6			

Score, MASCOT score; MW, molecular weight; Pep, peptide matches, number of peptides identified to protein; ooSCC, the SCC of oocytes; pmSCC, the SCC of cloned constructs; ooSCC/pmSCC, the ratio of peptides matches for the same protein in ooSCC and pmSCC. No ratio is given for proteins detected in only one spindle type.

 $\label{eq:Table 3}$  Effect of  $\it CLTC$  mRNA injection on cloned embryo development

Treatment	No. of oocytes activated	No. of 2- cell embryos (%)	No. of 4- cell embryos (%)	No. of Morulae developed (%)	No. of Blastocysts developed (%)	No. of embryos transferred	No. of recipient mothers	No. of day 19.5 fetuses (% of transferred embryos)
EDTA inj.	299	283 (94.6)	232 (77.6)	174 (58.2)	105 (35.1)	83	6	3 (3.6)
CLTC mRNA inj.	278	258 (92.8)	225 (80.9)	172 (61.9)	103 (37.1)	103	6	3 (2.9)